

# Spin-1 Atoms in Optical Superlattices: Single-Atom Tunneling and Entanglement

Andreas Wagner and Christoph Bruder

*Department of Physics, University of Basel, Klingelbergstrasse 82, 4056 Basel, Switzerland*

Eugene Demler

*Department of Physics, Harvard University, Cambridge, Massachusetts 02138, USA*

(Dated: December 20, 2011)

We examine spinor Bose-Einstein condensates in optical superlattices theoretically using a Bose-Hubbard Hamiltonian that takes spin effects into account. Assuming that a small number of spin-1 bosons is loaded in an optical potential, we study single-particle tunneling that occurs when one lattice site is ramped up relative to a neighboring site. Spin-dependent effects modify the tunneling events in a qualitative and quantitative way. Depending on the asymmetry of the double well different types of magnetic order occur, making the system of spin-1 bosons in an optical superlattice a model for mesoscopic magnetism. We use a double-well potential as a unit cell for a one-dimensional superlattice. Homogeneous and inhomogeneous magnetic fields are applied and the effects of the linear and the quadratic Zeeman shifts are examined. We also investigate the bipartite entanglement between the sites and construct states of maximal entanglement. The entanglement in our system is due to both orbital and spin degrees of freedom. We calculate the contribution of orbital and spin entanglement and show that the sum of these two terms gives a lower bound for the total entanglement.

PACS numbers: 03.75.Mn, 03.75.Lm, 03.75.Gg

## I. INTRODUCTION

Ultracold atoms can be trapped via the ac Stark effect in optical lattices, which are created by counterpropagating laser beams; in case there are only a few atoms per site they build up optical crystals. These systems offer a unique combination of experimental and theoretical accessibilities [1]. They can be manipulated with a very high degree of accuracy and versatility so that they serve as quantum simulators, i.e. they can be used to simulate complex problems in many-body physics. Ultracold atoms in optical lattices offer robust quantum coherence, a unique controllability and powerful read-out tools, such as time-of-flight measurements [2, 3] or fluorescence imaging [4].

Trapping ultracold atoms in conventional magnetic traps leads to frozen spin degrees of freedom such that the atoms behave effectively as spinless particles. If the atoms are trapped by optical means only, the atoms keep the extra spin degree of freedom and the Bose-Einstein condensate becomes a spinor condensate. The spinor degree of freedom on alkaline gases corresponds to the manifold of degenerate Zeeman hyperfine levels. The ground-state properties of spinor Bose-Einstein condensates in single traps were investigated in Refs. [5, 6].

We study the behavior of spin-1 atoms in optical superlattices, in particular, an optical lattice that is formed by overlapping two standing-wave laser fields with a commensurate wavelength ratio of 2. The resulting lattice is an array of optical traps with a double-well structure. We model the case when each double-well potential is filled with a small number of spin-1 bosons. Spin-1 bosonic atoms in a double-well potential can be described by a variant of the two-site Bose-Hubbard Hamiltonian [7].

This model allows examining the interplay between the kinetic energy (embodied by the tunneling strength between the sites) and the particle interaction (covered by the on-site interaction, i.e. the interaction within the wells). Furthermore, it is possible to include an energy offset between the sites, and the spin-1 Bose-Hubbard model additionally contains a term that incorporates spin-dependent interactions. This term penalizes high-spin configurations on individual lattice sites in the case of antiferromagnetic interaction between the atoms (e.g. for  $^{23}\text{Na}$ ) and low-spin configuration in the case of ferromagnetic interactions (e.g. for  $^{87}\text{Rb}$ ).

The two-site Bose-Hubbard model for spinless bosons can be used to describe the transfer of single Cooper pairs in small Josephson junctions, i.e. the physics of Cooper-pair staircases [8–10]. With ultracold atoms in optical superlattices this model was realized and was shown to give rise to a single-atom staircase [11–15]. This is achieved by monitoring the particle number in either of the wells for different values of the energy offset. In the case of small tunneling strength, the difference in the number of atoms in the two wells does not change smoothly when the energy offset is varied but is characterized by a step-like behavior. Jumps from one step to the next signal the tunneling of a single atom. In this paper, such single-atom staircases are examined for spinor condensates. Depending on the energy bias, different types of magnetic order occur, and the system of spin-1 bosons in an optical superlattice becomes a model for mesoscopic magnetism. A specific example of how this mesoscopic magnetism can be observed in experiments is presented in Fig. 1. This figure shows the difference between bosonic staircases for two spin-1 bosons for configurations with different total spins. If the total spin is  $S_{\text{tot}} = 2$ , the spins of the two

atoms are parallel and for antiferromagnetic interactions, as in the case of  $^{23}\text{Na}$ , being in the same well costs extra energy. Therefore the  $S_{\text{tot}} = 2$  configuration switches later (i.e. at higher energy offset) to the state with both atoms in the same well. In the ferromagnetic case (such as  $^{87}\text{Rb}$ ), the curves for  $S_{\text{tot}} = 0$  and  $S_{\text{tot}} = 2$  will be exchanged.

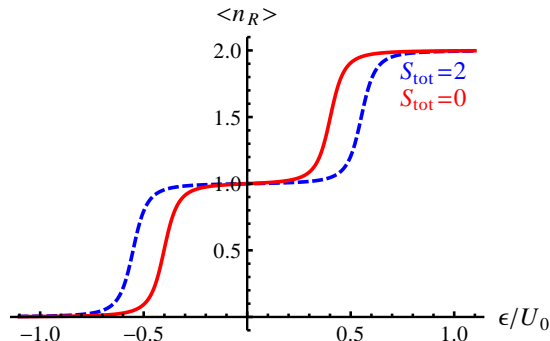


FIG. 1. (Color online) Two spin-1 bosons with antiferromagnetic ordering in a double-well potential. Here  $n_R$  is the occupation number of the right well, and  $\epsilon$  characterizes the energy offset between the two wells ( $t/U_0 = 0.05$  and  $U_2/U_0 = 0.1$ ). Depending on the total spin of the system, bosonic staircase transitions occur at different bias voltages. Note that both states with  $S_{\text{tot}} = 0$  (red, solid line) and  $S_{\text{tot}} = 2$  (blue, dashed line) have symmetric orbital wavefunctions with respect to particle exchange. The difference in the occupation numbers arises due to spin-dependent interactions and not due to a different orbital symmetry of the states. Thus, a measurement of the spin-dependent bosonic staircases provides a demonstration of mesoscopic magnetism.

Spin-1 atoms also allow stronger quantum correlations between the wells compared with the case of spinless bosons. For spinless bosons it has been noted that particle fluctuations between the left and the right well lead to entanglement between the wells (see e.g., Refs. [16, 17] and references therein). In addition to this orbital entanglement, spin-1 atoms allow spinor entanglement. In this paper, the quantum correlations between the wells are examined for different values of the energy offset and different ratios of the tunneling strength relative to the on-site interaction. We give a lower bound for the entanglement between the wells by estimating the amount of orbital and spinor entanglement separately. At this point, we consider entanglement mainly as a theoretical characterization of the many-body state of the system.

The paper is organized as follows: In Sec. II, the two-site Bose-Hubbard model for spin-1 atoms is introduced and is given explicitly for a small number of bosons. In Sec. III, the physics of the bosonic staircases is discussed, and in Sec. III C, the effect of magnetic fields is included. In Sec. IV, the bipartite entanglement for the two-site Bose-Hubbard model is examined. The total entanglement between the sites depends on orbital and spin degrees of freedom. We obtain a lower bound of the total

entanglement, which is given by the sum of the orbital entanglement and the spin entanglement.

## II. TWO-SITE BOSE-HUBBARD HAMILTONIAN FOR SPIN-1 ATOMS

The atoms we have in mind are alkali-metal atoms, such as  $^{23}\text{Na}$  and  $^{87}\text{Rb}$ . Degenerate gases of alkali-metal atoms are weakly interacting systems, but due to the confining lattice of counterpropagating laser beams some of the atoms are forced to be very close to each other and, thus, to become strongly interacting. Spin-1 bosonic atoms in a double-well potential can be described by a variant of the two-site Bose-Hubbard Hamiltonian [7, 18],

$$H_0 = \frac{U_0}{2} \sum_{i=L,R} n_i(n_i - 1) - t \sum_{\sigma} (\hat{L}_{\sigma}^{\dagger} \hat{R}_{\sigma} + \hat{R}_{\sigma}^{\dagger} \hat{L}_{\sigma}) + \varepsilon (n_L - n_R) + \frac{U_2}{2} \sum_{i=L,R} (\vec{S}_i^2 - 2n_i), \quad (1)$$

where  $\hat{L}_{\sigma}$  ( $\hat{L}_{\sigma}^{\dagger}$ ) and  $\hat{R}_{\sigma}$  ( $\hat{R}_{\sigma}^{\dagger}$ ) are annihilation (creation) operators for atoms in the hyperfine state  $\sigma \in \{-1, 0, 1\}$  in the left or right well and  $n_L = \sum_{\sigma} \hat{L}_{\sigma}^{\dagger} \hat{L}_{\sigma}$  ( $n_R = \sum_{\sigma} \hat{R}_{\sigma}^{\dagger} \hat{R}_{\sigma}$ ) is the atom number at the left (right) site. The annihilation and creation operators obey the canonical commutation relations  $[\hat{L}_i, \hat{L}_j^{\dagger}] = [\hat{R}_i, \hat{R}_j^{\dagger}] = \delta_{ij}$  and  $[\hat{R}_i, \hat{L}_j^{\dagger}] = [\hat{L}_i, \hat{R}_j^{\dagger}] = 0$ .  $\vec{S}_L = \sum_{\sigma\sigma'} \hat{L}_{\sigma}^{\dagger} \vec{T}_{\sigma\sigma'} \hat{L}_{\sigma'}$  is the total spin on the left site and the total spin on the right site is  $\vec{S}_R = \sum_{\sigma\sigma'} \hat{R}_{\sigma}^{\dagger} \vec{T}_{\sigma\sigma'} \hat{R}_{\sigma'}$ , where  $\vec{T}_{\sigma\sigma'}$  are the usual spin-1 matrices.

The on-site repulsive interaction is described by the first term in Eq. (1) and parametrized by  $U_0$ . The second term embodies the spin-symmetric tunneling between the wells and  $t$  is the hopping matrix element between the lattice sites;  $\varepsilon$  characterizes the difference in on-site energy between the sites. The term proportional to  $U_2$  describes spin-dependent interactions: It penalizes nonzero spin configurations on individual lattice sites in the case of antiferromagnetic interactions (e.g.,  $^{23}\text{Na}$ ) and favors high-spin configurations in the case of ferromagnetic interactions (e.g.,  $^{87}\text{Rb}$ ).

The parameters can be controlled by adjusting the intensity of the laser beams; it is possible to move from regimes of strong tunneling ( $U_0 \ll t$ ) to regimes of very weak tunneling ( $t \ll U_0$ ). For bulk lattices, it has been shown theoretically [18] and experimentally [19] that the system can be in a Mott-insulating regime (for  $t \ll U_0$ ) and in a superfluid phase, where the kinetic energy dominates (for  $U_0 \ll t$ ), and that it is possible to switch from one regime to the other by tuning the laser strength.

Whereas the ratio of  $U_0/t$  can be changed, the ratio  $U_0/U_2$  is fixed for all lattice geometries.  $U_2$  is given by the difference in the scattering length of two spin-1 bosons in the case that their spins couple to the total spin two, and the scattering length in the case that their spins couple

to the total spin zero. This leads to an estimated ratio of  $U_2/U_0 = 0.04$  for  $^{23}\text{Na}$  [7].

The Hamiltonian (1) conserves the particle number, the  $z$  projection of the total spin, i.e.  $(\vec{S}_L + \vec{S}_R)_z$ , and the total spin  $(\vec{S}_L + \vec{S}_R)^2$ . In each well the bosonic angular momenta couple, where symmetry constraints require  $n_i + S_i$  to be even, and the resulting spins of both wells couple to a total angular momentum  $\vec{S}_{tot} = \vec{S}_L + \vec{S}_R$ .

### A. Two spin-1 bosons

Since the hopping term in Eq. (1) conserves the absolute value of the total spin  $S_{tot} = |\vec{S}_L + \vec{S}_R|$ , the Hilbert space decomposes in orthogonal subspaces that do not mix, i.e.

$$\mathcal{H} = \mathcal{H}(S_{tot} = 0) \oplus \mathcal{H}(S_{tot} = 1) \oplus \mathcal{H}(S_{tot} = 2).$$

In the case of two spin-1 bosons, the Hilbert space is seven dimensional

$$\begin{aligned} |E_1\rangle &= |\{2, 0\}, \{0, 0\}, 0\rangle, \\ |E_2\rangle &= |\{1, 1\}, \{1, 1\}, 0\rangle, \\ |E_3\rangle &= |\{0, 2\}, \{0, 0\}, 0\rangle, \\ |E_4\rangle &= |\{1, 1\}, \{1, 1\}, 1\rangle, \\ |E_5\rangle &= |\{2, 0\}, \{2, 0\}, 2\rangle, \\ |E_6\rangle &= |\{1, 1\}, \{1, 1\}, 2\rangle, \\ |E_7\rangle &= |\{0, 2\}, \{0, 2\}, 2\rangle, \end{aligned}$$

using the notation  $|\{n_L, n_R\}, \{S_L, S_R\}, S_{tot}\rangle$ . These basis vectors belong to three orthogonal subspaces,

$$\mathcal{H} = \underbrace{\{E_1, E_2, E_3\}}_{S_{tot}=0} \oplus \underbrace{\{E_4\}}_{S_{tot}=1} \oplus \underbrace{\{E_5, E_6, E_7\}}_{S_{tot}=2}.$$

To examine the ground-state properties of this system the Hamiltonian needs to be calculated and diagonalized for each subspace separately. To calculate the off-diagonal elements of the Hamiltonian it is necessary to write the elements of the whole system as product of the single-well wavefunctions, e.g.,

$$|\{2, 0\}, \{2, 0\}, 2\rangle = |n_L = 2, S_L = 2, S_{1z} = 0\rangle \otimes |n_R = 0, S_R = 0, S_{2z} = 0\rangle$$

and

$$\begin{aligned} &|\{1, 1\}, \{1, 1\}, 2\rangle \\ &= \sum_{m=-1, 0, 1} C_{(1, m), (1, -m)}^{(2, 0)} |1, 1, m\rangle \otimes |1, 1, -m\rangle \\ &= \frac{1}{\sqrt{6}} (|1, 1, 1\rangle \otimes |1, 1, -1\rangle \\ &+ 2|1, 1, 0\rangle \otimes |1, 1, 0\rangle + |1, 1, -1\rangle \otimes |1, 1, 1\rangle) \end{aligned}$$

where we have chosen the  $S_z = 0$  component for convenience because the energy does not depend on the  $S_z$

component. The single-well wavefunctions need to be written in terms of single-particle creation operators. For two spin-1 bosons this can be performed using the standard Clebsch-Gordan coefficients.

The diagonal elements are given by

$$\begin{aligned} \langle E_1|H|E_1\rangle &= 2\epsilon + U_0 - 2U_2, \\ \langle E_3|H|E_3\rangle &= -2\epsilon + U_0 - 2U_2, \\ \langle E_5|H|E_5\rangle &= 2\epsilon + U_0 + U_2, \\ \langle E_7|H|E_7\rangle &= -2\epsilon + U_0 + U_2, \\ \langle E_2|H|E_2\rangle &= \langle E_4|H|E_4\rangle = \langle E_6|H|E_6\rangle = 0. \end{aligned}$$

Due to the conservation of the total angular momentum the Hamiltonian is block diagonal. The only nonvanishing tunneling elements are

$$\begin{aligned} \langle E_1|H|E_2\rangle &= \langle E_2|H|E_3\rangle = -\sqrt{2}t, \\ \langle E_5|H|E_6\rangle &= \langle E_6|H|E_7\rangle = -\sqrt{2}t. \end{aligned}$$

### B. Higher boson numbers

The Hilbert space for three spin-1 bosons is given by the direct sum of the following subspaces:

$$\mathcal{H} = \{E_1, E_2, E_3, E_4, E_5, E_6\} \oplus \{E_7, E_8\} \oplus \{E_9, E_{10}, E_{11}, E_{12}\}.$$

The subspace  $\{E_1, E_2, E_3, E_4, E_5, E_6\}$  belongs to  $|\vec{S}_L + \vec{S}_R| = 1$ , the subspace  $\{E_7, E_8\}$  belongs to  $|\vec{S}_L + \vec{S}_R| = 2$ , and the subspace  $\{E_9, E_{10}, E_{11}, E_{12}\}$  belongs to  $|\vec{S}_L + \vec{S}_R| = 3$ . The basis vectors are given by

$$\begin{aligned} |E_1\rangle &= |\{3, 0\}, \{1, 0\}, 1\rangle, \\ |E_2\rangle &= |\{2, 1\}, \{2, 1\}, 1\rangle, \\ |E_3\rangle &= |\{2, 1\}, \{0, 1\}, 1\rangle, \\ |E_4\rangle &= |\{1, 2\}, \{1, 2\}, 1\rangle, \\ |E_5\rangle &= |\{1, 2\}, \{1, 0\}, 1\rangle, \\ |E_6\rangle &= |\{0, 3\}, \{0, 1\}, 1\rangle, \\ |E_7\rangle &= |\{2, 1\}, \{2, 1\}, 2\rangle, \\ |E_8\rangle &= |\{1, 2\}, \{1, 2\}, 2\rangle, \\ |E_9\rangle &= |\{3, 0\}, \{3, 0\}, 3\rangle, \\ |E_{10}\rangle &= |\{2, 1\}, \{2, 1\}, 3\rangle, \\ |E_{11}\rangle &= |\{1, 2\}, \{1, 2\}, 3\rangle, \\ |E_{12}\rangle &= |\{0, 3\}, \{0, 3\}, 3\rangle, \end{aligned}$$

again using the notation  $|\{n_L, n_R\}, \{S_L, S_R\}, S_{tot}\rangle$ .

The Hamiltonian is block diagonal in the basis given above as in the case of two bosons. The Hamiltonians belonging to  $|\vec{S}_L + \vec{S}_R| = 2$  and  $|\vec{S}_L + \vec{S}_R| = 3$  are quite similar to the spinless case and the case of two spin-1 atoms. To calculate the off-diagonal elements of the Hamiltonian we need to know how  $n$  spin-1 bosons couple to a total spin  $\vec{S}$  with a  $z$ -projection  $S_z$ . For three spin-1 bosons

this is performed in the Appendix. The off-diagonal elements for  $|\vec{S}_L + \vec{S}_R| = 2$  and  $|\vec{S}_L + \vec{S}_R| = 3$  are

$$\begin{aligned}\langle E_7|H|E_8\rangle &= -t, \\ \langle E_9|H|E_{10}\rangle &= \langle E_{11}|H|E_{12}\rangle = -\sqrt{3}t, \\ \langle E_{10}|H|E_{11}\rangle &= -2t.\end{aligned}$$

The diagonal elements are given by

$$\begin{aligned}\langle E_7|H|E_7\rangle &= \langle E_{10}|H|E_{10}\rangle = U_0 + \epsilon + U_2, \\ \langle E_8|H|E_8\rangle &= \langle E_{11}|H|E_{11}\rangle = U_0 - \epsilon + U_2, \\ \langle E_9|H|E_9\rangle &= U_0 + 3\epsilon + 3U_2, \\ \langle E_{12}|H|E_{12}\rangle &= 3U_0 - 3\epsilon + 3U_2.\end{aligned}$$

The Hamiltonian belonging to the Hilbert space  $|\vec{S}_L + \vec{S}_R| = 1$  exhibits a richer structure and differs from the spinless case. This is because the term  $-t\sum_{\sigma}(L_{\sigma}^{\dagger}R_{\sigma} + R_{\sigma}^{\dagger}L_{\sigma})$  describes tunneling between several basis vectors, e.g. between  $|E_1\rangle$  and  $|E_2\rangle$  as well as between  $|E_1\rangle$  and  $|E_3\rangle$ . Because the energy does not depend on the  $S_z$  projection we can set  $S_z = 0$ . The basis vector  $|E_1\rangle$  is given by

$$\begin{aligned}|\{3,0\}, \{1,0\}, 1\rangle &= |3,1,0\rangle \otimes |0,0,0\rangle \\ &= \left[ \sqrt{\frac{2}{5}}\hat{L}_{-1}^{\dagger}\hat{L}_0^{\dagger}\hat{L}_1^{\dagger} - \sqrt{\frac{1}{10}}\left(\hat{L}_0^{\dagger}\right)^3 \right] |0\rangle,\end{aligned}$$

and the basis vector  $|E_2\rangle$  is given by

$$\begin{aligned}|\{2,1\}, \{2,1\}, 1\rangle &= \sum_{m=-2,\dots,2} \sum_{n=-1,0,1} C_{(1,m),(1,n)}^{(1,0)} |2,2,m\rangle \otimes |1,1,n\rangle \\ &= \sqrt{\frac{3}{10}}|2,1,-1\rangle \otimes |1,1,1\rangle - \sqrt{\frac{4}{10}}|2,1,0\rangle \otimes |1,1,0\rangle \\ &+ \sqrt{\frac{3}{10}}|2,1,1\rangle \otimes |1,1,-1\rangle \\ &= \left[ -\sqrt{\frac{2}{15}}\left(\hat{L}_0^{\dagger}\right)^2\hat{R}_0^{\dagger} + \sqrt{\frac{3}{10}}\hat{L}_1^{\dagger}\hat{L}_0^{\dagger}\hat{R}_{-1}^{\dagger} \right. \\ &+ \left. \sqrt{\frac{3}{10}}\hat{L}_{-1}^{\dagger}\hat{L}_0^{\dagger}\hat{R}_1^{\dagger} - \sqrt{\frac{2}{15}}\hat{L}_{-1}^{\dagger}\hat{L}_1^{\dagger}\hat{R}_0^{\dagger} \right] |0\rangle.\end{aligned}$$

Now, we can calculate the corresponding nondiagonal element of the Hamiltonian,

$$\langle E_1|H|E_2\rangle = -t \langle E_1| \sum_{\sigma} (\hat{L}_{\sigma}^{\dagger}\hat{R}_{\sigma} + \hat{R}_{\sigma}^{\dagger}\hat{L}_{\sigma}) |E_2\rangle = -\sqrt{\frac{5}{3}}t.$$

The basis vector  $|E_3\rangle$  is given by

$$\begin{aligned}|\{2,1\}, \{0,1\}, 1\rangle &= |2,0,0\rangle \otimes |1,1,0\rangle \\ &= \left[ \sqrt{\frac{2}{3}}\hat{L}_{-1}^{\dagger}\hat{L}_1^{\dagger}\hat{R}_0^{\dagger} - \frac{1}{\sqrt{6}}\left(\hat{L}_0^{\dagger}\right)^2\hat{R}_0^{\dagger} \right] |0\rangle,\end{aligned}$$

and the corresponding nondiagonal element of the Hamiltonian is

$$\langle E_1|H|E_3\rangle = -\sqrt{\frac{4}{3}}t.$$

Note that the off-diagonal elements of the Hamiltonian depend on the spin configurations, also, the off-diagonal elements do not depend on the strength of the spin-dependent interactions  $U_2$ . Similar calculations lead to the remaining off-diagonal elements,

$$\begin{aligned}\langle E_2|H|E_4\rangle &= -\frac{t}{3}, \\ \langle E_2|H|E_5\rangle &= \langle E_3|H|E_4\rangle = -\frac{2\sqrt{5}t}{3}, \\ \langle E_3|H|E_5\rangle &= -\frac{2t}{3}, \\ \langle E_4|H|E_6\rangle &= \langle E_1|H|E_2\rangle = -\sqrt{\frac{4}{3}}, \\ \langle E_5|H|E_6\rangle &= \langle E_1|H|E_3\rangle = -\sqrt{\frac{5}{3}}.\end{aligned}$$

The diagonal elements are given by

$$\begin{aligned}\langle E_1|H|E_1\rangle &= 3U_0 + 3\epsilon - 2U_2, \\ \langle E_2|H|E_2\rangle &= U_0 + \epsilon + U_2, \\ \langle E_3|H|E_3\rangle &= U_0 + \epsilon - 2U_2, \\ \langle E_4|H|E_4\rangle &= U_0 - \epsilon + U_2, \\ \langle E_5|H|E_5\rangle &= U_0 - \epsilon - 2U_2, \\ \langle E_6|H|E_6\rangle &= 3U_0 - 3\epsilon - 2U_2.\end{aligned}$$

Higher boson numbers lead to analogous expressions that are used in the following but are not given here.

### III. BOSONIC STAIRCASES

The two-site Bose-Hubbard model may be used to model Cooper-pair staircases [8–10] relevant for small Josephson junctions. In the case of ultracold atoms the same effect gives rise to single-atom staircases [11–15]. Here we present such staircases for spin-1 atoms.

#### A. General treatment

The Hilbert spaces decompose into different subspaces according to the total spin of the system. Different subspaces are not mixed by ramping up the energy difference between the double wells and behave in a different way. In the case of two bosons this is shown in Fig. 1. The different widths of the steps centered at  $\epsilon = 0$  correspond to different values of total spins per site. At  $\epsilon = 0.5$ , state  $|\{1,1\}, \{1,1\}, 2\rangle$  is energetically lower than state  $|\{0,2\}, \{0,2\}, 2\rangle$ , which makes the step broader for  $S_{tot} = 2$ . On the contrary, at  $\epsilon = 0.5$ , state  $|\{1,1\}, \{1,1\}, 0\rangle$  is energetically higher than state  $|\{0,2\}, \{0,0\}, 0\rangle$ , which makes the step narrower for  $S_{tot} = 0$ .

In general, depending on the sign of  $U_2$ , states with high single-well angular momenta get penalized or get favored. If  $U_2 > 0$  (such as, e.g., for  $^{23}\text{Na}$ ), nonzero

spin configurations get penalized. In the case of  $^{87}\text{Rb}$ ,  $U_2$  is negative and spin-dependent interactions lead to the opposite effect: High-spin configurations are favored, and the corresponding steps are broader. Therefore, in the ferromagnetic case, the curves for  $S_{tot} = 0$  and  $S_{tot}$  in Fig. 1 will be exchanged.

The exact position of the steps can be calculated in the atomic limit, i.e.,  $t = 0$ . The step positions generally depend linearly on  $U_2$ . For some spin configurations, e.g., odd atom number, lowest possible total spin, and antiferromagnetic interactions, the step positions do not depend on spin-dependent interactions.

For higher boson numbers, the richer structure of the off-diagonal elements means that the variance in the particle number depends on the total spin and the energy offset. In the case of three bosons (Fig. 2), the step at  $\epsilon = 0$  is not shifted due to symmetry reasons, whereas the steps at  $\epsilon = 1$  and  $\epsilon = -1$  are shifted linearly. At the same time, the steps belonging to  $S_{tot} = 3$  are not as sharp as the steps belonging to  $S_{tot} = 1$ , i.e., the curve of the variance in  $n_L$  is broader in the case of  $S_{tot} = 3$ .

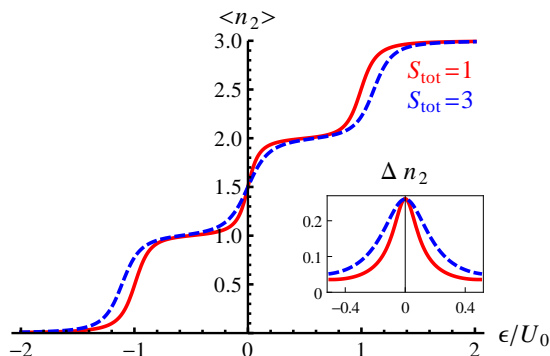


FIG. 2. (Color online) Bosonic staircase for three spin-1 bosons with antiferromagnetic ordering in a double-well potential ( $t/U_0 = 0.05$  and  $U_2/U_0 = 0.1$ ):  $S_{tot} = 1$  (red, solid line) and  $S_{tot} = 3$  (blue, dashed line). (Inset) Variance in the particle number in the left well for the step around  $\epsilon = 0$ .

The staircases for different total spins may be used to arrange spin-1 atoms in a two-dimensional (2D) superlattice according to their spin degrees of freedom (see Fig. 3).

## B. Beyond ground-state analysis

The gap between the ground state and the first excited state in the energy spectrum depends strongly on the tunneling between the sites (see Figs. 4 and 5). For finite temperatures the density matrix describing the system, thus, is highly mixed for small tunneling parameters, and the ground-state behavior only dominates if tunneling is sufficiently strong.

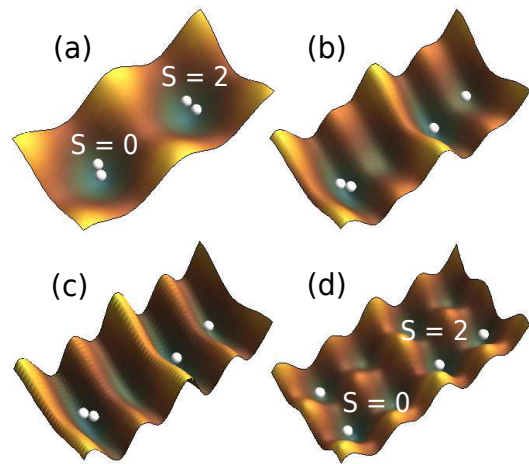


FIG. 3. (Color online) A possible way to separate the  $S_{tot} = 2$  spin component from the  $S_{tot} = 0$  spin component in the case of antiferromagnetic interactions between the atoms: The potentials in the  $x$  and  $y$  directions are manipulated separately. In the first step (b), the energy offset between the double wells is lifted until the bosons combining with the total spin  $S_{tot} = 0$  separate while the bosons belonging to  $S_{tot} = 2$  still remain in the same site. (c) Next, the wells are separated by a large potential barrier and tunneling is suppressed. (d) An additional laser is switched on and the bosons coupling to  $S_{tot} = 2$  distribute in the resulting double well. The switching is assumed to happen adiabatically such that the system can be regarded to be in the ground state at every instant.

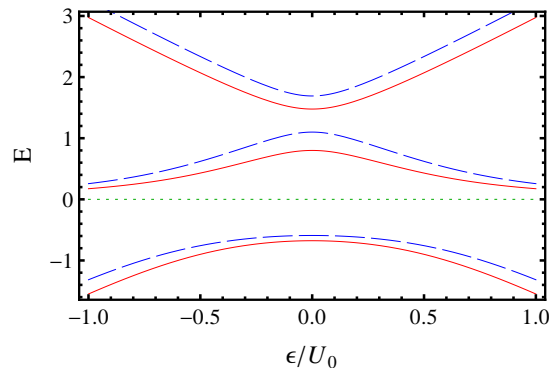


FIG. 4. (Color online) Energy spectrum of two spin-1 bosons in a double well with strong tunneling ( $t/U_0 = 0.5$  and  $U_2/U_0 = 0.1$ ):  $S_{tot} = 0$  subspace (red, solid lines),  $S_{tot} = 2$  (blue, dashed lines), and  $S_{tot} = 1$  (dotted line).

## C. Magnetic field included

The effect of a magnetic field can be included in the model (1) by adding a term to the Hamiltonian that describes the coupling of the spins to the magnetic field [20]. The first contribution of a magnetic field  $\vec{B} = (0, 0, B)$  is

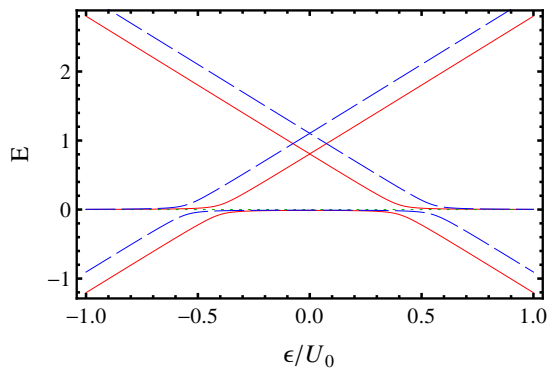


FIG. 5. (Color online) Energy spectrum of two spin-1 bosons in a double well with weak tunneling ( $t/U_0 = 0.05$  and  $U_2/U_0 = 0.1$ ). Color code as in Fig. 4.

a regular Zeeman shift in the energy levels:

$$H = H_0 + p \sum_{i=L,R} \sum_{\sigma} m_{i\sigma} \hat{n}_{i\sigma} = H_0 + p S_z^{tot}$$

where  $p = g\mu_B B$  and  $\hat{n}_{i\sigma}$  is the particle number operator for the  $i$ th site that gives the number of bosons in the  $m$ th hyperfine state. The linear Zeeman shift changes the overall state considerably. The energy eigenvalues belonging to  $S_{tot} \neq 0$  split into multiplets because the hyperfine levels are no longer degenerate (see Fig. 6). For

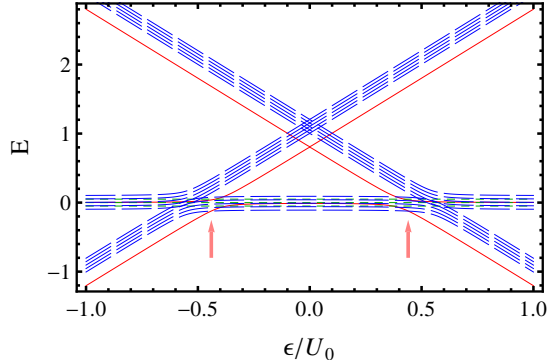


FIG. 6. (Color online) Linear Zeeman shift of the energy levels in the energy spectrum of two spin-1 bosons ( $B/U_0 = 0.05$ ,  $t/U_0 = 0.05$  and  $U_2/U_0 = 0.1$ ). The energy levels of Fig. 5 split into spin multiplets. The red arrows denote ground state level crossings. Color code as in Fig. 4.

a given tunneling strength, there is a critical magnetic-field strength that leads to ground-state level crossings. Such level crossings correspond to spin-flip transitions, i.e., the ground-state energy is continuous, but the expectation values of the particle number of single sites and of the magnetization are not. This means that the overall ground state of the system does not belong to the same  $z$  projection of the total spin for all values of the energy offset  $\epsilon$ . Figure 7 shows the critical value of the magnetic field in the case of two bosons.

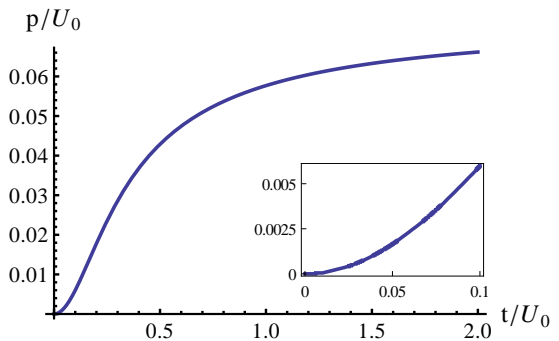


FIG. 7. (Color online) Critical magnetic field  $p = g\mu_B B$  above which the staircase for two bosons shows a discontinuous behavior signifying spin-flip transitions ( $U_2/U_0 = 0.1$ ).

However, spin-non-conserving collisions are negligible over the lifetime of the condensate, and the total magnetization is a conserved quantity on the time scale of the experiment [21, 22]. For a given magnetization the properties of the system are not altered by the linear Zeeman effect; the whole spectrum merely is shifted. Only if one is interested in comparing different magnetizations, the linear Zeeman effect has to be taken into account. In a series of experiments with a given magnetization, it is necessary, therefore, to include higher-order contributions in the magnetic field. The quadratic Zeeman effect arises because the hyperfine spins characterizing ultra-cold atoms are mixtures of electron and nuclear spins. Since the magnetic field approximately couples only to the electron spin, the Zeeman effect is nonlinear in the field but, typically, can be described by a sum of linear and quadratic terms.

For each of the subspaces belonging to different magnetizations  $S_z^{tot}$ , there is a separate effective Hamiltonian

$$H_q = H_0 + q \sum_{i=L,R} \sum_{\sigma} m_{i\sigma}^2 \hat{n}_{i\sigma}. \quad (2)$$

The magnitude of the quadratic Zeeman shift is given by  $q = q_0 B^2$ , where e.g.  $q_0 = h \times 390 \text{ Hz/G}^2$  for Na [21].

In the case of two bosons the system with magnetization  $S_z^{tot} = 0$  possesses the most interesting structure because the Hilbert space is composed of states with different total spins. For  $S_z^{tot} = 2$ , the quadratic Zeeman shift does not alter the staircase since it leads to a homogeneous shift in all the energy levels. The staircases at different magnetic fields are shown in Fig. 8. For  $S_z^{tot} = 0$ , the step positions depend in a nonlinear way on the magnetic field strength. It is no longer possible to read them off in the atomic limit (i.e.,  $t = 0$ ) because the existence of the quadratic Zeeman shift leads to additional nondiagonal elements in the Hamiltonian. Note that the quadratic Zeeman effect does not eliminate the difference in the two staircases, which is the main manifestation of mesoscopic magnetism.



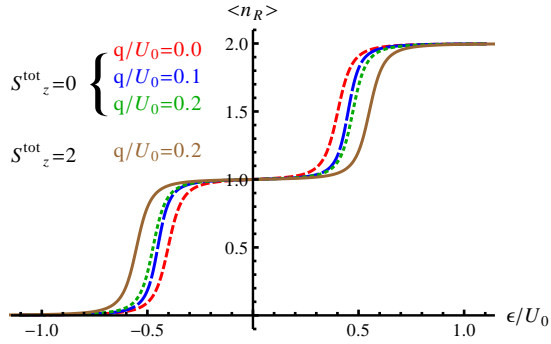


FIG. 8. (Color online) Two spin-1 bosons with antiferromagnetic ordering in a double-well potential ( $t/U_0 = 0.05$  and  $U_2/U_0 = 0.1$ ). (Dashed lines)  $S_z^{tot} = 0$  for different magnetic fields  $q = q_0 B^2$  (short dashes  $q/U_0=0.2$ , long dashes  $q/U_0=0.1$  and medium sized dashes  $q/U_0=0$ ). (Solid line)  $S_z^{tot} = 2$ . In this case the staircase does not depend on the magnetic field. The difference in this staircase to the ones with  $S_z^{tot} = 0$ , which is the main manifestation of mesoscopic magnetism, persists in the presence of the quadratic Zeeman effect.

Due to the fact that the quadratic Zeeman shift does not commute with the operator of the total spin  $S^{tot}$ , the eigenstates of the Hamiltonian given in Eq. (2) are no longer eigenstates of  $S_{tot}$ . For  $B \neq 0$ , the ground state of the system is a superposition of different eigenstates of  $S_{tot}$ , i.e., states with different  $S_{tot}$  hybridize (see Fig. 9). For certain values of the energy offset  $\epsilon$  (e.g.,  $\epsilon/U_0 = 1$  and  $\epsilon/U_0 = -1$  for four bosons), the appearance of a magnetic field changes the ground state strongly. This reflects the specific spin configurations.

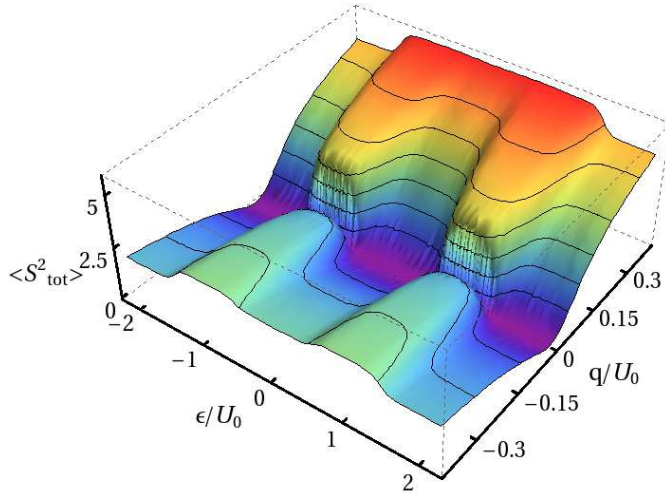


FIG. 9. (Color online) Expectation value  $\langle S_{tot}^2 \rangle$  of the system for four bosons for different magnetic fields  $q = q_0 B^2$  ( $S_z^{tot} = 0$ ,  $t/U_0 = 0.05$  and  $U_2/U_0 = 0.1$ ).

The quadratic Zeeman shift also changes the overall spectrum for a given magnetization qualitatively such

that, in the case of thermal occupation of the double well the density matrix of the system changes considerably. For  $q = 0$ , the ground state nearly is degenerate with the first excited state, whereas the gap widens for finite values of  $q$ .

Additionally one can include inhomogeneous magnetic fields,

$$H = H_q + \Delta B (S_{Lz} - S_{Rz}),$$

where  $\Delta B$  describes the strength of the field gradient. The magnetic-field offset  $\Delta B$  changes the Hamiltonian if  $S_{totz} \neq 0$ . For some configurations, e.g. two bosons in a double well,  $\Delta B$  merely leads to an overall shift in  $\epsilon$ , i.e., an inhomogeneous magnetic field is equivalent to an energy offset  $\epsilon$ . In general, this is not the case, and  $\Delta B$  is an additional tool to reshape the staircases depending on the spin configuration of the system.

#### IV. ENTANGLEMENT FOR SPIN-1 BOSONS

Entanglement is a unique feature of quantum-mechanical systems. Understanding entanglement deepens our understanding of quantum mechanics and, therefore, is of fundamental interest. Moreover, entanglement is a resource for quantum computation and correlates separated systems stronger than all classical correlations can do. For bipartite pure states entanglement is well understood and the different entanglement measures are equivalent. In the following we will use the entanglement of formation (EOF) [23] as an entanglement measure. The EOF is the number of Einstein-Podolsky-Rosen pairs asymptotically required to prepare a given state by local operations and classical communication. The entanglement of formation between two qudits ( $D$ -dimensional objects) in a pure state is given by the von Neumann entropy of the reduced density matrix of each single qudit [24]. To calculate the EOF, consider a system consisting of two parts labeled  $A$  and  $B$ . Any pure state  $|\Psi\rangle$  of the system can be written in the Schmidt decomposition [25]

$$|\Psi\rangle = \sum_i^D c_i |\psi_i^A\rangle \otimes |\psi_i^B\rangle,$$

where  $\{\psi_1^A, \dots, \psi_D^A\}$  and  $\{\psi_1^B, \dots, \psi_D^B\}$  are complete sets of orthonormal states of the respective subsystems. The system is entangled iff there is more than one nonvanishing coefficient  $c_i$ . These coefficients  $c_i$  are positive, unique and invariant under local operations and, therefore, can be used to quantify the entanglement between  $A$  and  $B$ . The von Neumann entropy of the reduced density matrix of each single qudit is given by

$$\begin{aligned} E(\Psi) &= S(\text{Tr}_B |\Psi\rangle\langle\Psi|) = S(\text{Tr}_A |\Psi\rangle\langle\Psi|) \\ &= - \sum_1^D c_i^2 \log_2 c_i^2, \end{aligned}$$

where  $S$  indicates the entropy. It ranges from zero to  $\log_2 D$ . The entanglement of formation of two qudits with  $D > 2$  thereby exceeds the entanglement of formation of two qubits, i.e. higher-dimensional objects contain more entanglement and violate all Clauser-Horne-Shimony-Holt-inequalities more strongly than qubits.

In the following we calculate the EOF in a double well and examine how much the two sites are entangled. At this point, we consider the EOF mainly as a theoretical characterization of the many-body state of the system.

The EOF for typical parameters is shown in Fig. 10. The maximal entanglement exceeds the maximal entan-

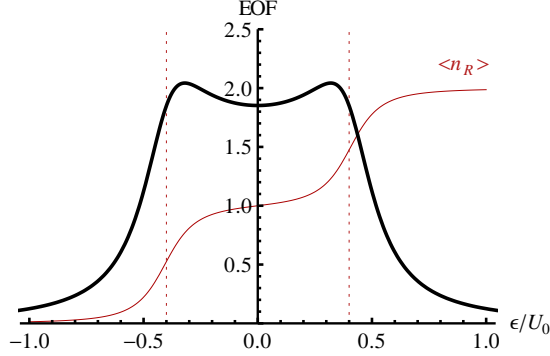


FIG. 10. (Color online) EOF between two wells for two bosons with antiferromagnetic interactions ( $t/U_0 = 0.1$  and  $U_2/U_0 = 0.1$ ) for the total spin  $S_{tot} = 0$ .

glement between two qutrits of  $\log_2 3 \approx 1.585$ . This is due to particle fluctuations. The total amount of entanglement stems from orbital and spin degrees of freedom.

Magnetic fields have a strong effect on the entanglement of formation. Figure 11 shows the EOF of four bosons at  $S_z^{tot} = 0$ . For  $q > 0$ , the contribution of the spin degrees of freedom to the entanglement of formation is suppressed already by small magnetic fields. This is somewhat surprising, because the system is constrained to  $S_z^{tot}$ , i.e. the state with the strongest spin entanglement of all states with a given total spin. For  $q < 0$ , this contribution initially is reduced but then remains constant as a function of  $q$ .

### A. Two spin-1 bosons

For two bosons and in the case of  $S_{tot} = 0$  a possible orthonormal basis is given by

$$\{\psi_1, \psi_2, \psi_3\} = \{|\{2, 0\}, \{0, 0\}, 0\rangle, |\{1, 1\}, \{1, 1\}, 0\rangle, |\{0, 2\}, \{0, 0\}, 0\rangle\}$$

using the notation  $|\{n_L, n_R\}, \{S_L, S_R\}, S_{tot}\rangle$ . The decomposition,

$$|\Psi\rangle = \sum_i^3 c_i |\psi_i\rangle$$

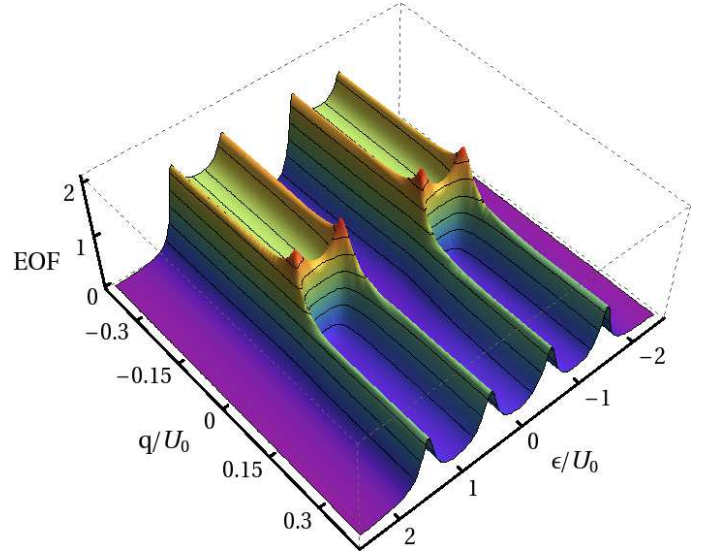


FIG. 11. (Color online) EOF between two wells for four particles in the presence of a magnetic field ( $S_z^{tot} = 0$ ,  $t/U_0 = 0.05$  and  $U_2/U_0 = 0.1$ ). For  $q > 0$ , even small fields will eliminate the contribution of the spin degrees of freedom to the entanglement.

is not a Schmidt decomposition, because the vector  $|\psi_2\rangle$  is a superposition of orthonormal states,

$$\begin{aligned} |\{1, 1\}, \{1, 1\}, 0\rangle &= -\frac{1}{\sqrt{3}}|1, 1, 0; 1, 1, 0\rangle \\ &+ \frac{1}{\sqrt{3}}|1, 1, 1; 1, 1, -1\rangle + \frac{1}{\sqrt{3}}|1, 1, -1; 1, 1, 1\rangle, \end{aligned}$$

using the notation  $|n_L, S_L, S_{Lz}; n_R, S_R, S_{Rz}\rangle$ . The entanglement of formation of  $|\psi_2\rangle$  is given by

$$E(|\psi_2\rangle) = 3\frac{1}{3} \log_2 3.$$

The EOF of  $|\Psi\rangle$  is given by

$$\begin{aligned} E(|\Psi\rangle) &= -c_1^2 \log_2 c_1^2 - c_3^2 \log_2 c_3^2 - 3 \left(c_2 \frac{1}{\sqrt{3}}\right)^2 \log_2 \left(c_2 \frac{1}{\sqrt{3}}\right)^2 \\ &= -\sum_i^3 c_i^2 \log_2 c_i^2 + c_2^2 \log_2 3 \\ &= -\sum_i^3 c_i^2 \log_2 c_i^2 + \sum_i^3 c_i^2 E(|\psi_i\rangle) \\ &= E_{\text{orbital}} + E_{\text{spin}}. \end{aligned} \tag{3}$$

The total entanglement between the left and the right well decomposes in an orbital part and a spin part. The orbital part stems from the coefficients that distinguish different orbital wave functions. The spin part originates from the EOF of the individual basis vectors, each



weighted with the coefficient  $c_i^2$ . The coefficients  $c_i$  depend on the tunneling strength  $t$ , on the on-site interaction  $U_0$ , on the spin-dependent interaction  $U_2$ , and on the energy offset  $\varepsilon$ .

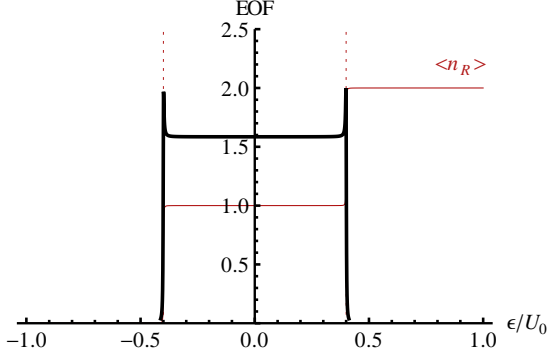


FIG. 12. (Color online) EOF between two wells for two bosons with very weak tunneling and antiferromagnetic interactions ( $t/U_0 = 0.001$  and  $U_2/U_0 = 0.1$ ) for the total spin  $S_{tot} = 0$ .

In the limit of weak tunneling  $t \ll U_0$  the Hamiltonian is diagonal in the basis  $\{\psi_1, \psi_2, \psi_3\}$  and the ground state of a symmetric double-well potential (i.e.  $\varepsilon = 0$ ) is given by

$$|\Psi_0\rangle = |\psi_2\rangle = -\frac{1}{\sqrt{3}}|1, 1, 0; 1, 1, 0\rangle + \frac{1}{\sqrt{3}}|1, 1, 1; 1, 1, -1\rangle + \frac{1}{\sqrt{3}}|1, 1, -1; 1, 1, 1\rangle, \quad (4)$$

which leads to an entanglement of  $E(|\psi_2\rangle) = \log_2 3$ , see Fig. 12.

In the limit of strong tunneling (i.e.  $U_0 \ll t$ ), the ground state of the system is

$$|\Psi_0\rangle = \frac{1}{2}|\psi_1\rangle + \frac{1}{\sqrt{2}}|\psi_2\rangle + \frac{1}{2}|\psi_3\rangle. \quad (5)$$

For this state the orbital entanglement is given by  $E_{\text{orbital}} = -2\frac{1}{4}\log_2 \frac{1}{4} - \frac{1}{2}\log_2 \frac{1}{2} = 3/2$  and the spin entanglement is given by  $E_{\text{spin}} = \left(\frac{1}{\sqrt{2}}\right)^2 \log_2 3 \approx 0.792$ . Therefore, the total entanglement is  $E(|\Psi_2\rangle) \approx 2.292$ . This is not the maximum amount of entanglement that can be obtained for this system (see Fig. 13). The maximal entanglement is not the sum of the maximal qutrit entanglement and the maximal orbital entanglement because the orbital motion leads to particle number fluctuations and reduces the spin entanglement (see Fig. 14). The maximal orbital entanglement is realized in the limit of strong tunneling; the maximal spin entanglement corresponds to the maximally localized state, i.e.,  $|\psi_2\rangle$ .

### B. Three spin-1 bosons

The EOF between the two sites is presented in Fig. 15 for  $t/U_0 = 0.1$  and in Fig. 16 for very weak tunneling. In

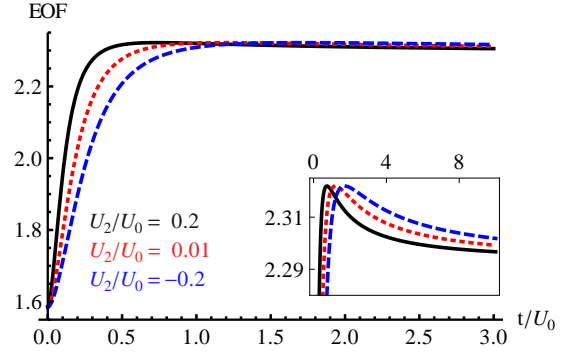


FIG. 13. (Color online) EOF between two symmetric wells ( $\varepsilon = 0$ ) for different values of  $U_2$ , i.e., different spin interactions (solid line  $U_2/U_0 = 0.2$ , dotted line  $U_2/U_0 = 0.01$ , and dashed line  $U_2/U_0 = -0.2$ ).

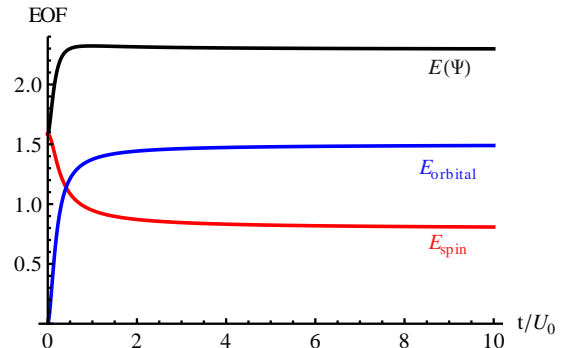


FIG. 14. (Color online) EOF,  $E_{\text{spin}}$  and  $E_{\text{orbital}}$  between two symmetric wells for  $U_2/U_0 = 0.1$ .

contrast to the case of two bosons, in the weak-tunneling case the system is not entangled for large intervals of the energy offset  $\varepsilon$ .

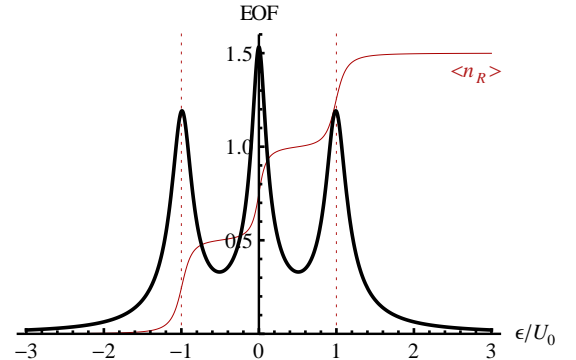


FIG. 15. (Color online) EOF between two wells for three bosons with antiferromagnetic interactions ( $t/U_0 = 0.1$  and  $U_2/U_0 = 0.1$ ) for the total spin  $S_{tot} = 1$ .

To quantify this effect, we analyze the EOF again in detail. The spins  $\vec{S}_L$  and  $\vec{S}_R$  couple to a total spin, for

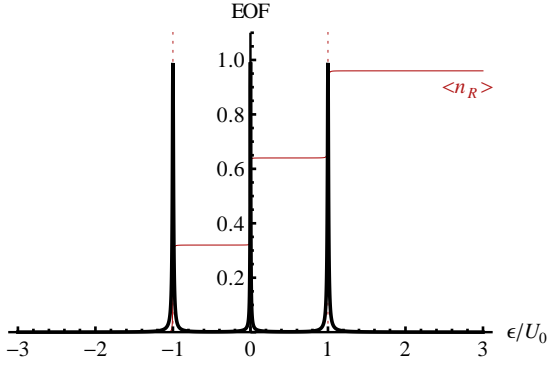


FIG. 16. (Color online) EOF between two wells for three bosons with antiferromagnetic interactions ( $t/U_0 = 0.005$  and  $U_2/U_0 = 0.1$ ) for the total spin  $S_{tot} = 1$ .

which three absolute values are possible,  $S_{tot} \in \{1, 2, 3\}$ .

It is obvious that Eq. (3) is applicable for  $S_{tot} = 2$  and  $S_{tot} = 3$ . The interesting case is  $S_{tot} = 1$ . Each state with quantum number  $S_{tot} = 1$  can be written as

$$|\Psi\rangle = \sum_i^6 c_i |\psi_i\rangle. \quad (6)$$

Only two of the basis vectors contain true spin entanglement,

$$\begin{aligned} |\psi_2\rangle &= |((2, 1), (2, 1), 1)\rangle = \alpha|2, 2, 0; 1, 1, 0\rangle \\ &\quad + \beta|2, 2, 1; 1, 1, -1\rangle + \gamma|2, 2, -1; 1, 1, 1\rangle \\ |\psi_4\rangle &= |((1, 2), (1, 2), 1)\rangle = \alpha|1, 1, 0; 2, 2, 0\rangle \\ &\quad + \beta|1, 1, 1; 2, 2, -1\rangle + \gamma|1, 1, -1; 2, 2, 1\rangle \end{aligned}$$

with  $\alpha = -\sqrt{\frac{2}{5}}$  and  $\beta = \gamma = \sqrt{\frac{3}{10}}$ . Any superposition of  $|\psi_2\rangle$  and  $|\psi_3\rangle$  can be written as

$$\begin{aligned} c_2|\psi_2\rangle + c_3|\psi_3\rangle &= \sqrt{c_2^2\alpha^2 + c_3^2} |L\rangle \otimes |1, 1, 0\rangle_R \\ &\quad + c_2\beta|2, 2, 1; 1, 1, -1\rangle + c_2\gamma|2, 2, -1; 1, 1, 1\rangle \end{aligned} \quad (7)$$

where  $|L\rangle$  is the normalized function  $1/\sqrt{c_2^2\alpha^2 + c_3^2} (c_2\alpha|2, 2, 0\rangle_L + c_3|2, 0, 0\rangle_L)$ , which is orthogonal to the other vectors appearing in Eqs. (7) and (6). Therefore, the decomposition Eq. (7) is a Schmidt decomposition and the full entanglement of formation of  $|\Psi\rangle$  can be calculated,

$$\begin{aligned} E(|\Psi\rangle) &= -c_1^2 \log_2 c_1^2 - (c_2^2\alpha^2 + c_3^2) \log_2 (c_2^2\alpha^2 + c_3^2) \\ &\quad - (c_2^2\beta^2) \log_2 (c_2^2\beta^2) - (c_2^2\gamma^2) \log_2 (c_2^2\gamma^2) \\ &\quad - (c_4^2\alpha^2 + c_5^2) \log_2 (c_4^2\alpha^2 + c_5^2) - (c_4^2\beta^2) \log_2 (c_4^2\beta^2) \\ &\quad - (c_4^2\gamma^2) \log_2 (c_4^2\gamma^2) - c_6^2 \log_2 c_6^2. \end{aligned} \quad (8)$$

It is possible to decompose the entanglement into different contributions and to generalize the expressions for

$E_{\text{orbital}}$  and  $E_{\text{spin}}$  in Eq. (3). To calculate the orbital entanglement we construct the orbital wave function and use this to get the EOF of the reduced density matrix. The orbital wave function is

$$\begin{aligned} |\Psi\rangle_{\text{orbital}} &= \\ c_1|3, 0\rangle &+ \sqrt{c_2^2 + c_3^2}|2, 1\rangle + \sqrt{c_4^2 + c_5^2}|1, 2\rangle + c_6|0, 3\rangle, \end{aligned}$$

where the quantum numbers refer to  $|n_L, n_R\rangle$ . So the orbital entanglement of formation between the left and the right well is given by

$$\begin{aligned} E_{\text{orbital}} &= -c_1^2 \log_2 c_1^2 - (c_2^2 + c_3^2) \log_2 (c_2^2 + c_3^2) \\ &\quad - (c_4^2 + c_5^2) \log_2 (c_4^2 + c_5^2) - c_6^2 \log_2 c_6^2 \end{aligned} \quad (9)$$

The spin wave function is given by

$$\begin{aligned} |\Psi\rangle_{\text{spin}} &= \sqrt{c_1^2 + c_5^2} |\{1, 0\}, 1\rangle + c_2 |\{2, 1\}, 1\rangle \\ &\quad + \sqrt{c_3^2 + c_6^2} |\{0, 1\}, 1\rangle + c_4 |\{1, 2\}, 1\rangle, \end{aligned} \quad (10)$$

where the quantum numbers refer to  $|\{S_L, S_R\}, S_{tot}\rangle$ . The EOF of these orthonormal basis vectors is  $E(|\{1, 0\}, 1\rangle) = E(|\{0, 1\}, 1\rangle) = 0$  and  $E(|\{2, 1\}, 1\rangle) = E(|\{1, 2\}, 1\rangle) = -\alpha^2 \log_2 \alpha^2 - \beta^2 \log_2 \beta^2 - \gamma^2 \log_2 \gamma^2$ . Therefore, the EOF due to spin entanglement is

$$E_{\text{spin}} = c_2^2 E(|\psi_2\rangle) + c_4^2 E(|\psi_4\rangle). \quad (11)$$

Note that

$$\begin{aligned} &(c_2^2\alpha^2 + c_3^2) \log_2 (c_2^2\alpha^2 + c_3^2) + (c_2^2\beta^2) \log_2 (c_2^2\beta^2) \\ &\quad + (c_2^2\gamma^2) \log_2 (c_2^2\gamma^2) \\ &\leq c_3^2 \log_2 (c_2^2 + c_3^2) + (c_2^2) \log_2 \left(1 + \frac{c_3^2}{c_2^2}\right) \\ &\quad + c_2^2 \log_2 c_2^2 - c_2^2 E(|\psi_2\rangle) \\ &= (c_2^2 + c_3^2) \log_2 (c_2^2 + c_3^2) - c_2^2 E(|\psi_2\rangle), \end{aligned} \quad (12)$$

where  $\log(1 + dz) \leq d \log(1 + z)$  for  $d \geq 1$  and  $z \geq 0$  has been used. Because of Eq. (12) the entanglement of formation is bounded from below (see Fig. 17),

$$E(|\Psi\rangle) \geq E_{\text{orbital}} + E_{\text{spin}} \quad (13)$$

### C. Arbitrary number of bosons

Let  $\Psi$  be a wave function that describes the state of  $N$  bosons. This wave function can be written in terms of a basis, which is ordered according to the occupation numbers  $N_L$  and  $N_R$ , the spin in the left well  $S_L$  and the spin in the right well  $S_R$ , and the total spin  $S_{tot}$ ;

$$|\Psi\rangle = \sum_{n=1}^D c_n |\phi_n\rangle, \quad (14)$$

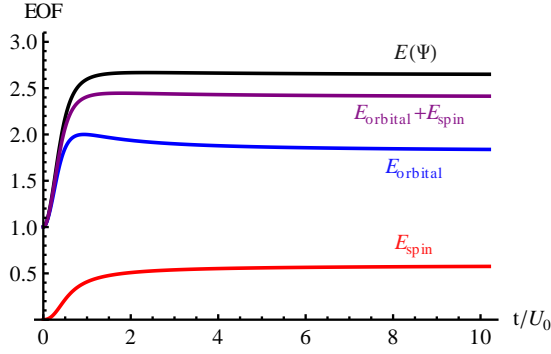


FIG. 17. (Color online) EOF,  $E_{\text{spin}}$ ,  $E_{\text{orbital}}$  and  $E_{\text{spin}} + E_{\text{orbital}}$  between two symmetric wells for three bosons with antiferromagnetic interactions ( $U_2/U_0 = 0.1$ ) in a symmetric double-well potential ( $\varepsilon/U_0 = 0$ ).

where  $\sum_n c_n^2 = 1$  and  $D \geq N$  is the dimension of the basis. We can rearrange this sum by sorting it according to the occupation numbers,

$$|\Psi\rangle = \sum_{m=0}^N |\psi_m\rangle,$$

where  $|\psi_m\rangle$  is the part of the wave function belonging to  $N_L = m$ . If  $N(m)$  is the number of basis vectors belonging to  $N_L = m$ ,  $|\psi_m\rangle$  is given by

$$|\psi_m\rangle = \sum_{i=1}^{N(m)} c(m)_i |\phi(m)_i\rangle, \quad (15)$$

where  $\sum_{i=1}^{N(m)} c(m)_i^2 \leq 1$  and  $c(m)_i$  denote the coefficients  $c_i$  that belong to  $N_L = m$ . Now it is possible to generalize Eqs. (9) and (11) and to define the orbital EOF,

$$E_{\text{orbital}} = - \sum_{m=0}^N \sum_{i=1}^{N(m)} c(m)_i^2 \log_2 \sum_{i=1}^{N(m)} c(m)_i^2 \quad (16)$$

and the spin EOF

$$E_{\text{spin}} = \sum_{n=1}^D c_n^2 E(|\phi_n\rangle). \quad (17)$$

It is not necessary to specify which basis vectors in Eq. (14) belong to which angular momentum configuration, such as in Eq. (10) because the total spin-entanglement entropy can be written as a sum over all basis vectors.

In this section we prove that Eq. (13) is true for any number of bosons in a double well:

$$E(|\Psi\rangle) \geq E_{\text{orbital}} + E_{\text{spin}}. \quad (18)$$

$E(|\Psi\rangle)$  decomposes in a sum over  $m$ :  $E(|\Psi\rangle) = \sum_m^N E(|\psi_m\rangle)$ . It is possible to write down the EOF for

each  $|\psi_m\rangle$  in the following way:

$$E(|\psi_m\rangle) = - \sum_j \left( \sum_i \alpha(m)_{ij}^2 c(m)_i^2 \right) \log_2 \left( \sum_i \alpha(m)_{ij}^2 c(m)_i^2 \right), \quad (19)$$

which defines a basis for each vector  $\phi(m)_i$ ,

$$\begin{aligned} |\phi(m)_i\rangle &= \sum_k \sum_l a(m)_{ik} a(m)_{il} |L_k\rangle \otimes |R_l\rangle \\ &= \sum_j \alpha(m)_{ij} |L, R\rangle_j, \end{aligned}$$

where  $\sum_j \alpha_{ij}^2 = 1$ . To prove Eq. (18) for any number of bosons, it is necessary and sufficient to show that Eq. (18) is true for each  $E(|\psi_m\rangle)$ , i.e.,

$$\begin{aligned} &\sum_j \left( \sum_i \alpha_{ij}^2 c_i^2 \right) \log_2 \left( \sum_i \alpha_{ij}^2 c_i^2 \right) \\ &\leq \left( \sum_i c_i^2 \right) \log_2 \left( \sum_i c_i^2 \right) + \sum_i c_i^2 \sum_j \alpha_{ij}^2 \log_2 \alpha_{ij}^2. \end{aligned} \quad (20)$$

The term on the left-hand side can be rearranged,

$$\begin{aligned} &\sum_j \left( \sum_i \alpha_{ij}^2 c_i^2 \right) \log_2 \left( \sum_i \alpha_{ij}^2 c_i^2 \right) \\ &= \sum_j \sum_i (\alpha_{ij}^2 c_i^2) \log_2 (\alpha_{ij}^2 c_i^2) \\ &\quad + \sum_j \sum_i (\alpha_{ij}^2 c_i^2) \log_2 \left( \frac{\sum_n \alpha_{nj}^2 c_n^2}{\alpha_{ij}^2 c_i^2} \right), \end{aligned} \quad (21)$$

as well as the term on the right-hand side,

$$\begin{aligned} &\left( \sum_i c_i^2 \right) \log_2 \left( \sum_i c_i^2 \right) + \sum_i c_i^2 \sum_j \alpha_{ij}^2 \log_2 \alpha_{ij}^2 \\ &= \left( \sum_i c_i^2 \right) \log_2 \left( \sum_i c_i^2 \right) - \sum_i c_i^2 \log_2 c_i^2 \\ &\quad + \sum_i \sum_j (\alpha_{ij}^2 c_i^2) \log_2 (\alpha_{ij}^2 c_i^2). \end{aligned}$$

Note that, due to Jensen's inequality,

$$\begin{aligned} &\sum_j (\alpha_{ij}^2 c_i^2) \log_2 \left( \frac{\sum_n \alpha_{nj}^2 c_n^2}{\alpha_{ij}^2 c_i^2} \right) \\ &\leq c_i^2 \log_2 \left( \frac{\sum_j \sum_n \alpha_{nj}^2 c_n^2}{c_i^2} \right) \\ &= c_i^2 \log_2 \left( \sum_n c_n^2 \right) - c_i^2 \log_2 c_i^2, \end{aligned}$$

Eq. (20) is fulfilled and, therefore, Eq. (18).

### D. Comparison with the entanglement of particles

The amount of entanglement shared between two parties might be lowered by superselection rules [26]. In case two parties share  $N$  particles and a particle superselection rule applies, the extractable bipartite entanglement, i.e., the degree of entanglement one can entangle two initially not entangled quantum registers located at  $A$  and  $B$ , is given by the entanglement of particles [27],

$$E_P(|\Psi_{AB}\rangle) \equiv \sum_n P_n E(|\Psi_{AB}^{(n)}\rangle),$$

where  $|\Psi_{AB}^{(n)}\rangle$  is  $|\Psi_{AB}\rangle$  projected onto the subspace of fixed local particle number, i.e.,  $n$  particles for one party and  $n-1$  for the other.

The entanglement of particles for two bosons in a double well is given by  $E_{\text{spin}}$  in Eq. (3). For three bosons the case  $S_{\text{tot}} = 2$  and  $S_{\text{tot}} = 3$  is trivial, but the case  $S_{\text{tot}} = 1$  is more interesting and is examined. To calculate  $E_P$ , we write down the projection obeying local particle superselection rules. The projections onto  $n_L = 3$  and  $n_L = 0$  are trivial and do not contribute to  $E_P$ . The projection onto  $n_L = 2$  leads to Eq. (7) with  $P_2 = c_2^2 + c_3^2$ . The entanglement contained in this state is given by

$$E(|\Psi_{LR}^{(2)}\rangle) = -\frac{c_2^2\alpha^2 + c_3^2}{c_2^2 + c_3^2} \log_2 \frac{c_2^2\alpha^2 + c_3^2}{c_2^2 + c_3^2} - \frac{c_2^2\beta^2}{c_2^2 + c_3^2} \log_2 \frac{c_2^2\beta^2}{c_2^2 + c_3^2} - \frac{c_2^2\gamma^2}{c_2^2 + c_3^2} \log_2 \frac{c_2^2\gamma^2}{c_2^2 + c_3^2}$$

and thereby contributes

$$P_2 E|\Psi_{LR}^{(2)}\rangle = -(c_2^2\alpha^2 + c_3^2) \log_2 (c_2^2\alpha^2 + c_3^2) - (c_2^2\beta^2) \log_2 (c_2^2\beta^2) - (c_2^2\gamma^2) \log_2 (c_2^2\gamma^2) + (c_2^2 + c_3^2) \log_2 (c_2^2 + c_3^2)$$

to  $E_P$ . A comparison with Eq. (8) shows that the equation,

$$E(|\Psi\rangle) = E_{\text{orbital}} + E_P \quad (22)$$

holds for three bosons. This equation also is true for higher boson numbers. The contribution of the state (15) to  $E_P$  is given by

$$P_m E|\Psi_{LR}^{(m)}\rangle = -\sum_j \left( \sum_i \alpha(m)_{ij}^2 c(m)_i^2 \right) \log_2 \left( \sum_i \alpha(m)_{ij}^2 c(m)_i^2 \right) + \left( \sum_i c(m)_i^2 \right) \log_2 \left( \sum_i c(m)_i^2 \right)$$

A comparison with Eq. (16) shows that Eq. (22) indeed holds for all boson numbers.

The necessity to take a superselection rule into account may arise due to several reasons. In some cases the phase between states with different local particle occupation

numbers is not well defined [28]. Consider the bipartite state

$$|\psi_\theta\rangle_{AB} = \sqrt{\frac{1}{2}} (|1, 0\rangle + e^{i\phi}|0, 1\rangle). \quad (23)$$

In case there is no shared reference frame and no tunneling between the two parties the phase is not accessible experimentally and the state is indistinguishable from an incoherent mixture,

$$\rho_{AB} = \frac{1}{2} (|1, 0\rangle\langle 1, 0| + |0, 1\rangle\langle 0, 1|). \quad (24)$$

Whenever one is concerned with the occupation number of massive particles, the detailed properties of the system determine which local operations and classical communication (LOCCs) are allowed: If tunneling is forbidden, LOCCs will conserve the local particle number. In this case a local particle number superselection rule must be taken into account. A more trivial example is the case of a superselection rule for the total particle number [29].

In our model (1) the phase is well defined due to the finite-tunneling amplitude. The amount of orbital entanglement  $E_{\text{orbital}}$  depends directly on the particle fluctuations caused by the tunneling between the sites. In the absence of tunneling, the orbital entanglement vanishes and the superselection rule for the local particle number is effectively enforced.

### E. Creation of entanglement structures

In the case of two spin-1 bosons in a double well the state of total spin zero ( $S_{\text{tot}} = |\vec{S}_L + \vec{S}_R| = 0$ ) is singled out. First, it can be separated from the  $S_{\text{tot}} = 2$  state due to a different particle distribution within the double well in the vicinity of the single-particle tunneling resonance (i.e.  $\epsilon/U_0 = 0.5$ ). Second, it represents the two-qutrit singlet state and thereby contains the maximal qutrit entanglement of  $\log_2 3$ . This distinguishes the qutrit entanglement from the qubit entanglement where the singlet state and the triplet ( $S_{\text{tot}})_z = 0$  state contain the same amount of entanglement.

This can be used to create specific entanglement structures in 2D optical superlattices (see Fig. 3).

## V. CONCLUSION

We have analyzed the two-site Bose-Hubbard model for spin-1 atoms explicitly for small numbers of bosons. Starting from the explicit form of the Hamiltonian, we have discussed the physics of the bosonic staircases. We also have studied the effect of magnetic fields. In the following we have examined the bipartite entanglement for the two-site Bose-Hubbard model. We have analyzed the contribution of orbital and spin degrees of freedom and have derived a lower bound of the total entanglement, which is the sum of the orbital entanglement and

the spin entanglement. We compared the entanglement of particles and thereby elucidated the meaning of orbital entanglement and of superselection rules for the local particle number.

The staircases for different total spins establish a correspondence of the spatial motion and the spin configuration. Because the  $S_{tot} = 0$  singlet state of two bosons does contain more entanglement than the other eigenstates of the system this correspondence can be used to construct an entanglement witness in the system: In case one detects the typical spatial behavior of the  $S_{tot} = 0$  state, one can conclude to have its entanglement. With the help of fluorescence imaging, it is also possible to depopulate doubly occupied sites in the lattice and thereby to build a spin filter.

We have discussed entanglement between the sites, not the entanglement between the individual atoms. Even for an occupancy of one, i.e. one atom per site, these are different quantities, because the bosons are indistinguishable. Recently it was proposed to measure the entanglement between (spinless) bosons in an optical lattice [29] by standard time-of-flight measurements. Such measurements do not preserve the information about the entanglement between the individual sites. There are other possibilities for examining these systems experimentally. First, it is possible to estimate the entanglement by measurements of the atom positions because these correspond to specific spin configurations as we have demonstrated. These atom positions can be determined by standard time-of-flight measurements or direct fluorescence detection of individual sites [4]. Furthermore, it is possible to detect the spin configurations directly in a nondemolishing way with the help of the quantum Faraday effect [30]. Furthermore, it may be possible to relate the entanglement to additional observable experimental quantities, such as magnetization fluctuations in one of the wells, in analogy to what has been discussed for noninteracting particles [31]. We plan to explore this question in future papers.

## VI. ACKNOWLEDGMENTS

We would like to thank R. Fazio and T.L. Schmidt for discussions. This paper was financially supported by

the Army Research Office with funding from the DARPA OLE program, Harvard-MIT CUA, NSF Grant No. DMR-07-05472, AFOSR Quantum Simulation MURI, AFOSR MURI on Ultracold Molecules, and the ARO-MURI on Atomtronics, and by the the Swiss SNF, the NCCR Nanoscience, and the NCCR Quantum Science and Technology.

## Appendix A: Coupling of $n$ spin-1 bosons

The coupling of two spin-1 atoms is given in standard textbooks. The coupling of  $n$  spin-1 atoms to a total spin  $\tilde{S}$  with a  $z$ -projection  $S_z$  in terms of  $n$  single spins  $S_{iz}$  is calculated by the diagonalization of  $\tilde{S}^2$ .

For three spin-1 atoms we give the connection of the basis vectors ordered according to  $S_{iz}$  and the basis vectors ordered according to  $S$  and  $S_z$ ,

$$\begin{aligned}
|S = 3, S_z = 3\rangle &= |0_{-1}, 0_0, 3_1\rangle, \\
|S = 3, S_z = 2\rangle &= |0_{-1}, 1_0, 2_1\rangle, \\
|S = 3, S_z = 1\rangle &= (2|0_{-1}, 2_0, 1_1\rangle + |1_{-1}, 0_0, 2_1\rangle)/\sqrt{5}, \\
|S = 3, S_z = 0\rangle &= \sqrt{\frac{2}{5}}|0_{-1}, 3_0, 0_1\rangle + \sqrt{\frac{3}{5}}|1_{-1}, 1_0, 1_1\rangle, \\
|S = 3, S_z = -1\rangle &= (2|1_{-1}, 2_0, 0_1\rangle + |2_{-1}, 0_0, 1_1\rangle)/\sqrt{5}, \\
|S = 3, S_z = -2\rangle &= |2_{-1}, 1_0, 0_1\rangle, \\
|S = 3, S_z = -3\rangle &= |3_{-1}, 0_0, 0_1\rangle, \\
|S = 1, S_z = 1\rangle &= (-|0_{-1}, 2_0, 1_1\rangle + 2|1_{-1}, 0_0, 2_1\rangle)/\sqrt{5}, \\
|S = 1, S_z = 0\rangle &= -\sqrt{\frac{3}{5}}|0_{-1}, 3_0, 0_1\rangle + \sqrt{\frac{2}{5}}|1_{-1}, 1_0, 1_1\rangle, \\
|S = 1, S_z = -1\rangle &= (-|1_{-1}, 2_0, 0_1\rangle + 2|2_{-1}, 0_0, 1_1\rangle)/\sqrt{5}
\end{aligned}$$

- 
- [1] I. Bloch, J. Dalibard, and W. Zwerger, Rev. Mod. Phys. **80**, 885 (Jul 2008)
  - [2] F. Gerbier, S. Trotzky, S. Fölling, U. Schnorrberger, J. D. Thompson, A. Widera, I. Bloch, L. Pollet, M. Troyer, B. Capogrosso-Sansone, N. V. Prokof'ev, and B. V. Svistunov, Phys. Rev. Lett. **101**, 155303 (Oct 2008)
  - [3] P. Pedri, L. Pitaevskii, S. Stringari, C. Fort, S. Burger, F. S. Cataliotti, P. Maddaloni, F. Minardi, and M. Inguscio, Phys. Rev. Lett. **87**, 220401 (Nov 2001)
  - [4] J. F. Sherson, C. Weitenberg, M. Endres, M. Cheneau, I. Bloch, and S. Kuhr, Nature **467**, 68 (Sep 2010)
  - [5] T.-L. Ho, Phys. Rev. Lett. **81**, 742 (Jul 1998)
  - [6] T. Ohmi and K. Machida, Journal of the Physical Society of Japan **67**, 1822 (1998)
  - [7] A. Imambekov, M. Lukin, and E. Demler, Phys. Rev. A **68**, 063602 (Dec 2003)
  - [8] D. V. Averin, A. B. Zorin, and K. K. Likharev, Sov. Phys. JETP **61**, 407 (1985)
  - [9] P. Lafarge, H. Pothier, E. R. Williams, D. Esteve,

- C. Urbina, and M. H. Devoret, *Z. Phys. B: Condens. Matter* **85**, 327 (1991)
- [10] P. Lafarge, P. Joyez, D. Esteve, C. Urbina, and M. H. Devoret, *Nature* **365**, 422 (1993)
- [11] R. Gati and M. K. Oberthaler, *Journal of Physics B: Atomic, Molecular and Optical Physics* **40**, R61 (2007)
- [12] D. V. Averin, T. Bergeman, P. R. Hosur, and C. Bruder, *Phys. Rev. A* **78**, 031601 (Sep 2008)
- [13] P. Cheinet, S. Trotzky, M. Feld, U. Schnorrberger, M. Moreno-Cardoner, S. Fölling, and I. Bloch, *Phys. Rev. Lett.* **101**, 090404 (Aug 2008)
- [14] G. Ferrini, A. Minguzzi, and F. W. J. Hekking, *Phys. Rev. A* **78**, 023606 (Aug 2008)
- [15] M. Rinck and C. Bruder, *Phys. Rev. A* **83**, 023608 (Feb 2011)
- [16] G. Mazzaella, L. Salasnich, A. Parola, and F. Toigo, *Phys. Rev. A* **83**, 053607 (May 2011)
- [17] L. Dell'Anna, arXiv:1108.6188(2011)
- [18] D. Jaksch, C. Bruder, J. I. Cirac, C. W. Gardiner, and P. Zoller, *Phys. Rev. Lett.* **81**, 3108 (Oct. 1998)
- [19] M. Greiner, O. Mandel, T. Esslinger, T. Hänsch, and I. Bloch, *Nature* **415**, 39 (2002)
- [20] A. Imambekov, M. Lukin, and E. Demler, *Phys. Rev. Lett.* **93**, 120405 (Sep 2004)
- [21] J. Stenger, S. Inouye, D. M. Stamper-Kurn, H.-J. Miesner, A. P. Chikkatur, and W. Ketterle, *Nature* **396**, 345 (1998)
- [22] K. Rodriguez, A. Argüelles, A. K. Kolezhuk, L. Santos, and T. Vekua, *Phys. Rev. Lett.* **106**, 105302 (Mar 2011)
- [23] S. Popescu and D. Rohrlich, *Phys. Rev. A* **56**, R3319 (Nov 1997)
- [24] K. A. Dennison and W. K. Wootters, *Phys. Rev. A* **65**, 010301 (Dec 2001)
- [25] R. Horodecki, P. Horodecki, M. Horodecki, and K. Horodecki, *Reviews of Modern Physics* **81**, 865 (2009)
- [26] S. D. Bartlett and H. M. Wiseman, *Phys. Rev. Lett.* **91**, 097903 (Aug 2003)
- [27] H. M. Wiseman and J. A. Vaccaro, *Phys. Rev. Lett.* **91**, 097902 (Aug 2003)
- [28] M. R. Dowling, A. C. Doherty, and H. M. Wiseman, *Phys. Rev. A* **73**, 052323 (May 2006)
- [29] M. Cramer, M. B. Plenio, and H. Wunderlich, *Phys. Rev. Lett.* **106**, 020401 (Jan 2011)
- [30] K. Eckert, O. Romero-Isart, M. Rodriguez, M. Lewenstein, E. S. Polzik, and A. Sanpera, *Nat. Phys.* **4**, 50 (2008)
- [31] H. F. Song, C. Flindt, S. Rachel, I. Klich, and K. Le Hur, *Phys. Rev. B* **83**, 161408 (Apr 2011)